Reliability Engineering and System Safety 123 (2014) 63–72

Contents lists available at ScienceDirect

Reliability Engineering and System Safety

journal homepage: www.elsevier.com/locate/ress

Prognostics of lumen maintenance for High power white light emitting diodes using a nonlinear filter-based approach

Jiajie Fan [a,*], Kam-Chuen Yung [a], Michael Pecht [b]

[a] PCB Technology Center, Department of Industrial and Systems Engineering, The Hong Kong Polytechnic University, Hung Hom, Hong Kong
[b] Center for Advanced Life Cycle Engineering, University of Maryland, College Park, MD 20742, USA

ARTICLE INFO

Article history:
Received 23 May 2013
Received in revised form
11 October 2013
Accepted 17 October 2013
Available online 26 October 2013

Keywords:
High power white LEDs
Lumen maintenance
Prognostic-based qualification
Nonlinear filter
Recursive Unscented Kalman Filter

ABSTRACT

High power white light emitting diodes (HPWLEDs), with advantages in terms of luminous efficacy, energy saving, and reliability, have become a popular alternative to conventional luminaires as white light sources. Like other new electronic products, HPWLEDs must also undergo qualification testing before being released to the market. However, most traditional qualification tests, which require all devices under testing to fail, are time-consuming and expensive. Nowadays, as recommended by the Illuminating Engineering Society (IES, IES-TM-21-11), many LED manufacturers use a projecting approach based on short-term collected light output data to predict the future lumen maintenance (or lumen lifetime) of LEDs. However, this projecting approach, which depends on the least-square regression method, generates large prediction errors and uncertainties in real applications. To improve the prediction accuracy, we present in this paper a nonlinear filter-based prognostic approach (the recursive Unscented Kalman Filter) to predict the lumen maintenance of HPWLEDs based on the short-term observed data. The prognostic performance of the proposed approach and the IES-TM-21-11 projecting approach are compared and evaluated with both accuracy- and precision-based metrics.

© 2013 Elsevier Ltd. All rights reserved.

1. Introduction

High power white light emitting diodes (HPWLEDs), which are a next-generation green lighting source, are a novel technology which uses semiconductor materials to convert electricity into light [1,2]. Compared to traditional lighting sources (such as incandescent lamps, halogen incandescent lamps, and cold cathode fluorescent lamps), HPWLEDs have attracted increasing interest in the field of lighting systems owing to their high efficiency, environmental benefits, and long lifetime in applications. They have been widely used as a light source of indoor lighting, street lamps, advertising displays, decorative lighting, and monitor backlights [3,4].

Qualification testing is an essential procedure for certifying a new product and technology before being released to the market. For electronic products, manufacturers usually apply some electronic industry standards from the IPC-Association Connecting Electronics Industries and the Joint Electron Devices Engineering Council (JEDEC) to qualify their reliability. The LED industry also has its own qualification standards from the Illuminating Engineering Society (IES) [5,6], the American National Standards Institute/American National Standard Lighting Group (ANSI/ANSLG) [7,8] and The International Commission for Illumination (*Commission Internationale del' Eclairage*, CIE). However, most of these techniques are time-consuming and expensive, especially for devices with long lifetimes (such as HPWLEDs with more than 50,000 h lifetime, if thermal management techniques are well performed).

From the previous studies [9,10], lumen degradation is known as one of the two dominant wearout failure modes in HPWLEDs. Usually, the LED lumen lifetime is measured based on the lumen maintenance, which can be defined as the remaining percentages of initial light output over time [11]. The Alliance for Solid-State Illumination Systems and Technologies (ASSIST) recommends two LED lumen lifetimes based on the time to 50% light output degradation (L50: for display lighting) or 70% light output degradation (L70: for general lighting) at room temperature [12]. To predict the lumen maintenance (or lumen lifetime) of LEDs, a projecting approach based on the least-square regression method is now recommended by IES (IES-TM-21-11 [11]) and is also widely accepted by many LED manufacturers. For instance, Philips Lumileds [13] and CREE [14] are implementing this projecting approach to predict the lumen maintenance of LEDs in their reliability test reports. However, this projecting approach, depending on least-square regression, introduces large prediction errors and uncertainties.

Prognostics and health management (PHM) is a technique used for fault diagnostics and reliability predictions in electronics-rich components or systems [15]. To shorten a qualification test time for a highly reliable electronic device (such as HPWLEDs), we have imported prognostics into this test and build a prognostics-based

* Corresponding author. Tel.: +852 276 666 35.
E-mail address: jay.fan@connect.polyu.hk (J. Fan).

0951-8320/$ - see front matter © 2013 Elsevier Ltd. All rights reserved.
http://dx.doi.org/10.1016/j.ress.2013.10.005

qualification test. To reduce the prediction errors and uncertainties introduced by the IES-TM-21-11 projecting approach, a nonlinear filter-based prognostic approach (recursive Unscented Kalman Filter (UKF)) was used in this paper to predict the lumen maintenance of HPWLEDs based on the shot-term observed data.

The remainder of this paper is organized into four sections. Section 2 reviews the nonlinear filter approaches which are used for prognostics. Section 3 describes the device under testing (DUT) and experimental procedure. Section 4 introduces the IES-TM-21-11 projecting approach and the inference of UKF algorithms. Both the prognostic results and the evaluation of prognostic performances of two proposed approaches are then shown in Section 5. Finally, we present a conclusion in Section 6.

2. Literature review

Filtering has become one of the most widely used prognostic approaches for estimating and predicting the state of electronic components or systems based on a state-space model [16–18]. The most well-known filter is the Kalman filter (KF), which is considered to be an effective method of conducting linear state-space estimation with additive Gaussian noise [19,20]. However, for most nonlinear cases, KF will lose its efficacy. Therefore, it is essential to establish a nonlinear filter to solve prognostic problems in nonlinear systems.

Up to now, there have been some approximate nonlinear filters, such as the Extended Kalman Filter (EKF), the Particle Filter (PF) [21], and UKF, which have been used to deal with nonlinear problems. Among them, the EKF uses a first order Taylor approximation to linearize both the state and measurement models. The PF approximates the state distribution using a set of discrete, weighted samples, called particles. The UKF approach was first proposed by Julier et al. and developed by Wan et al. [22–24] to estimate the state of nonlinear systems by using a deterministic sampling approach (sigma point sampling) to capture the mean and covariance estimates with a minimal set of sample points.

Among these three nonlinear filters (Fig. 1), both EKF and UKF rely on the Gaussion approximation and use mean and covariance to represent a probabilistic distribution. Therefore, they have difficulties in dealing with non-Gaussian problems (i.e. multimodal distributions or probabilistic distributions with heavy tail). While PF is a class of nonlinear filters which do not require any assumption to the probabilistic distribution. It is based on the Sequential Monte Carlo (SMC) simulation method and uses a set of particles to approximate the posterior distribution. Thus, PF often provides better results for highly nonlinear/non-Gaussian systems. And it is much more effective than both EKF and UKF in solving problems with multimodal uncertainty distributions. However, with a large number of particles, the PF algorithm may be impractical to a real-time application in high-dimensional systems due to its high computational cost [25]. According to the different probabilistic characteristics of both state model and measurement model, Table 1 summarizes the application ranges of three nonlinear filter algorithms.

Compared to the other two nonlinear state estimation methods, UKF possesses many advantages in Gaussian systems: first, UKF eliminates the calculation of Jacobian and Hessian matrices in EKF and makes the estimation procedure easier; second, it increases the estimation accuracy by considering at least the second order Taylor expansion; third, it reduces computational cost by developing an optimal sampling approach (sigma point sampling); whereas the Monte Carlo random sampling approach used in PF does not. Several previous literature studies have shown that the UKF has been considered to be a useful approach for state-space prognostics and estimations for nonlinear systems. Santhanagopalan et al. [27] implemented the UKF method in the estimation of the state of charge for lithium ion cells. Lall et al. applied the UKF algorithm to

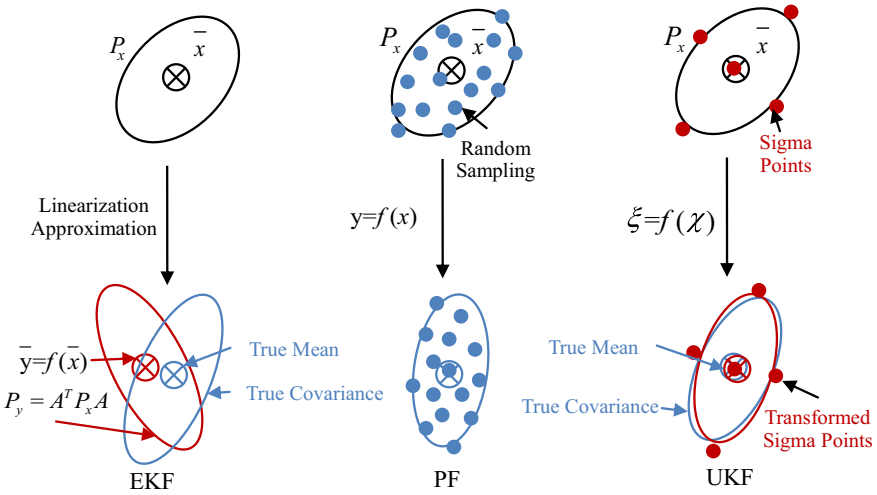

Fig. 1. Comparison of filter algorithms (EKF, PF and UKF) for prognostics.

Table 1
Application ranges of three nonlinear filter algorithms [26].

Measurement model	State model			
	Linear, Gaussian	Linear, non-Gaussian	Nonlinear, Gaussian	Nonlinear, non-Gaussian
Linear, Gaussian	KF	PF	EKF/UKF/PF	PF
Linear, Non-Gaussian	PF	PF	PF	PF
Nonlinear, Gaussian	EKF/UKF/PF	PF	EKF/UKF/PF	PF
Nonlinear, Non-Gaussian	PF	PF	PF	PF

predict the remaining useful life of electronic systems under mechanical shock and vibration conditions [28]. Jafarzadeh et al. [29] developed a UKF-based approach to estimate the nonlinear state of induction motor drives.

Considering the HPWLEDs' nonlinear characteristics in the lumen degradation process [10], in this paper, we present a UKF-based prognostic approach to predict the lumen maintenance based on the observed data. First, we modeled the lumen maintenance degradation process by using a nonlinear exponential model. Then the UKF approach was utilized to predict the future lumen maintenance based on observed data. Finally, the prognostic performances between the proposed UKF approaches and the IES-TM-21-11 projecting approach were evaluated and compared using both accuracy- and precision-based metrics.

3. Device under test and experimental procedure

3.1. Device under test

We selected one type of HPWLED from Philips Lumileds, the White LUXEON Rebel, which has high luminous flux (> 100 lm in cool white at 350 mA) [30]. Fig. 2 shows the packaging structure and luminescence mechanism of the White LUXEON Rebel. The mechanism of generating white light is a combination of blue light emitted by a GaN-based chip and the excited emission from YAG: Ce phosphor [31–33].

3.2. Experimental procedure

The experimental procedure included ten cycles for 10,000 h of operation. Each cycle involved three steps: aging, cooling, and testing (Fig. 3). For aging, twenty white LUXEON Rebel units were soldered onto a reliability test board that was thermally controlled by water cooling. The units were driven by a constant DC current in a thermal chamber. After 1000 h of aging, the reliability test board was removed from the thermal chamber to be cooled to room temperature. For testing, the lumen flux, chromaticity coordinates,

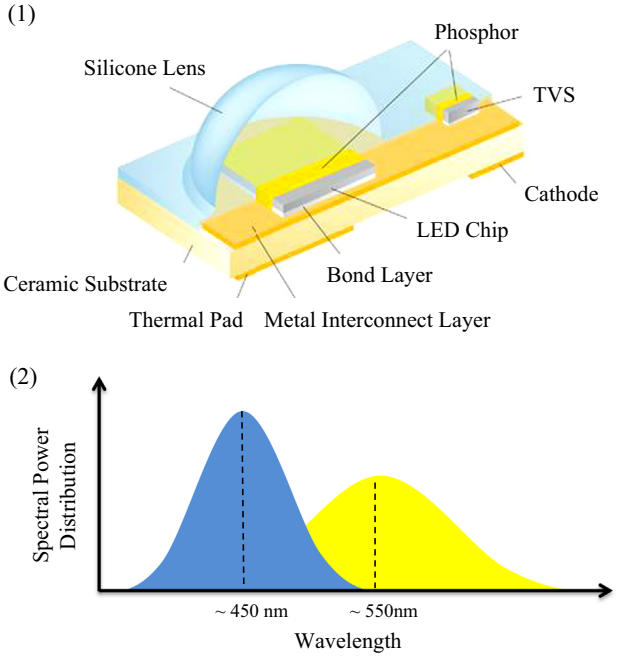

Fig. 2. White LUXEON Rebel packaging structure (1) and its luminescence mechanism (2).

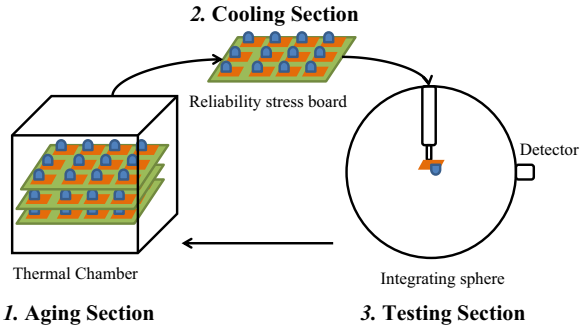

Fig. 3. Experimental procedure.

and forward voltage of each unit were measured underneath the integrating sphere. After testing, the reliability stress board was returned to the thermal chamber to undergo the next aging cycle. This study selected the lowest stress aging conditions from the LM-80 test report [34] (a driven current I_F of 350 mA and an aging temperature of 55 °C), which was the condition most similar to normal operation. Other high stress aging conditions will be considered in future accelerated testing work.

4. Models and methodologies

4.1. Lumen maintenance projecting approach

As recommended by IES-TM-21-11, the lumen maintenance data collected from the IES-LM-80-08 test report are fitted with a curve and then the curve is extrapolated to the given future time points(i.e., 10,000 h, 25,000 h, and 35,000 h) [11]. The operation procedure can be specified as follows:

4.1.1. Step 1: normalization

Normalize all collected lumen flux data to 1 (with the initial lumen maintenance value defined as 100%) at the time zero test point for each test unit. As mentioned before, lumen maintenance, *LM*, can be defined as the maintained percentages of initial light output over time:

$$LM(t) = \frac{\Phi(t)}{\Phi(0)} \times 100\% \quad (1)$$

where $\Phi(0)$ is the initial light output and $\Phi(t)$ is the lumen flux at time t.

4.1.2. Step 2: curve-fitting

The general degradation path model can be registered as time-performance measurement pairs (t_{i1}, LM_{i1}), (t_{i2}, LM_{i2}),…, (t_{ij}, LM_{ij}), for $i = 1, 2, \ldots\ldots, n$ (n is sample size); and j represents the test time points for each unit. The performance measurement for the ith unit at the jth test time is referred to as LM_{ij}. To estimate reliability by modeling the degradation data with the general degradation path model, Lu and Meeker [35] first proposed a mixed-effect model which assumes A_i is a fixed effect parameter representing the initial lumen maintenance of the ith unit; B_i is the degradation rate, a random effect parameter, which varies from unit to unit according to the diverse material properties of the different units and their production processes or handing conditions (Fig. 4).

Previous work on high power white LEDs indicated that the degradation trajectory of lumen performance followed an exponential curve [36,37]. Therefore, this study applied the LED exponential lumen degradation path model (Eq. (2)) to fit the lumen maintenance data for each unit and estimated the parameters of the

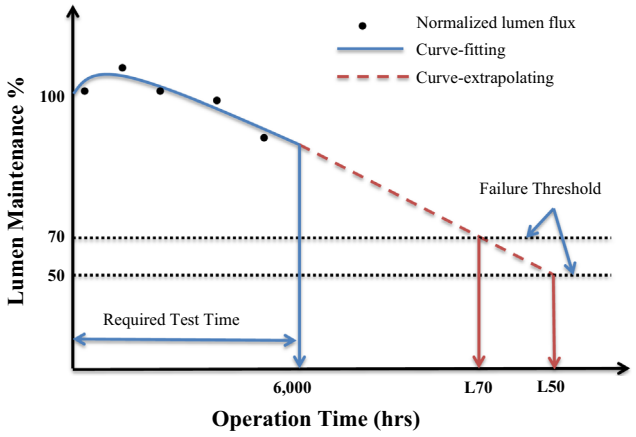

Fig. 4. IES-TM-21-11projecting approach.

model using the least squares method.

$$LM(t) = A_i \cdot \exp(-B_i \cdot t) \tag{2}$$

4.1.3. Step 3: curve-extrapolating

We extrapolate the curves based on the obtained parameters of the ith unit to get the future lumen maintenance data and project the lumen maintenance life L_p:

$$\text{For the } i\text{th } a \text{ unit} \quad L_p = \ln\left(\frac{100 \times A_i}{p}\right)/B_i \tag{3}$$

where p is the maintained percentage of the initial lumen output (i.e. 50, 70 recommended by ASSIST [12]).

4.2. Unscented Kalman Filter

The UKF algorithm involves estimation of the state of a discrete-time nonlinear dynamic system, which can be represented by both a state model and a measurement model:

$$\text{State model } x_k = f_k(x_{k-1}, v_{k-1}) \tag{4}$$

$$\text{Measurement model } y_k = h_k(x_k, n_k) \tag{5}$$

where x_k represents the unobserved state of the system, y_k is the observed measurements, v_{k-1} and n_k are the state noise and observation noise, respectively, and $v_{k-1} \sim N(0, Q_{k-1})$ and $n_k \sim N(0, R_k)$ are assumed to be the mean zero white Gaussian noises.

This study uses two types of UKF to predict the long-term lumen maintenance of HPWLEDs, augmented UKF, and non-augmented UKF. The algorithm implementations of these two UKFs can be expressed as follows:

4.2.1. Augmented UKF

4.2.1.1. Step 1: initialization. The initial state is described by its mean and covariance:

$$\bar{x}_0 = E[x_0] \tag{6}$$

$$P_0 = E[(x_0 - \bar{x}_0) \cdot (x_0 - \bar{x}_0)^T] \tag{7}$$

Supposing that both noises are non-additive, the initial state vector and covariance matrix can be expressed as an augment vector:

$$\bar{x}_0^a = E[x_0^a] = \begin{bmatrix} \bar{x}_0^T & 0 & 0 \end{bmatrix}^T \tag{8}$$

$$P_0^a = \begin{bmatrix} P_0 & 0 & 0 \\ 0 & Q_0 & 0 \\ 0 & 0 & R_0 \end{bmatrix} \tag{9}$$

4.2.1.2. Step 2: sigma point sampling. To undergo a nonlinear transformation, we develop a matrix χ_k^a with $2n_a+1$ sigma points

$$\chi_{k-1}^a = [\bar{x}_{k-1}^a \;\; \bar{x}_{k-1}^a + \sqrt{n_a+\lambda} \cdot \sqrt{p_{k-1}^a} \;\; \bar{x}_{k-1}^a - \sqrt{n_a+\lambda} \cdot \sqrt{p_{k-1}^a}] \tag{10}$$

$$n_a = n_x + n_v + n_n \tag{11}$$

$$\lambda = \alpha^2(n_a + k) - n_a \tag{12}$$

Then the sigma points are weighted by

$$W_0^{(m)} = \frac{\lambda}{n_a+\lambda} \tag{13}$$

$$W_0^{(c)} = \frac{\lambda}{n_a+\lambda} + (1 - \alpha^2 + \beta) \tag{14}$$

$$W_i^{(m)} = W_i^{(c)} = \frac{1}{2(n_a+\lambda)} \quad i = 1, 2, \ldots, 2n_a \tag{15}$$

where λ is the composite scaling parameter, which can be calculated from Eq. (12). The constant α determines the spread of sigma points around the mean ($1 \geq \alpha \geq 10^{-4}$); κ is a secondary scaling parameter which is usually set to $3-n_a$; and β is used to incorporate prior knowledge of the distribution of the state vector x (for Gaussian distribution, $\beta=2$). Here, we set $\alpha=0.01$, $\kappa = 3-n_a$, and $\beta=0$.

4.2.1.3. Step 3: time update. We estimate the transient state $\bar{x}_{k/k-1}$ and measurement $\bar{y}_{k/k-1}$:

$$\chi_{k/k-1}^x = f(\chi_{k-1}^x, \chi_{k-1}^v) \tag{16}$$

$$\bar{x}_{k/k-1} = \sum_{i=0}^{2n_a} W_i^{(m)} \chi_{i,k/k-1}^x \tag{17}$$

$$P_{k/k-1} = \sum_{i=0}^{2n_a} W_i^{(c)} [(\chi_{i,k/k-1}^x - \bar{x}_{k/k-1}) \cdot (\chi_{i,k/k-1}^x - \bar{x}_{k/k-1})^T] \tag{18}$$

$$y_{k/k-1} = h(\chi_{k/k-1}^x, \chi_{k-1}^n) \tag{19}$$

$$\bar{y}_{k/k-1} = \sum_{i=0}^{2n_a} W_i^{(m)} y_{i,k/k-1} \tag{20}$$

4.2.1.4. Step 4: measurement update. We calculate the cross-covariance of the state and measurement $P_{k/k-1}^{xy}$ and the Kalman gain K_k and compute the predicted mean $\bar{x}_k$ and covariance P_k.

$$P_{k/k-1}^{yy} = \sum_{i=0}^{2n_a} W_i^{(c)} [(y_{i,k/k-1} - \bar{y}_{k/k-1}) \cdot (y_{i,k/k-1} - \bar{y}_{k/k-1})^T] \tag{21}$$

$$P_{k/k-1}^{xy} = \sum_{i=0}^{2n_a} W_i^{(c)} [(\chi_{i,k/k-1}^x - \bar{x}_{k/k-1}) \cdot (y_{i,k/k-1} - \bar{y}_{k/k-1})^T] \tag{22}$$

$$K_k = P_{k/k-1}^{xy} (P_{k/k-1}^{yy})^{-1} \tag{23}$$

$$\bar{x}_k = \bar{x}_{k/k+1} + K_k(y_k - \bar{y}_{k/k-1}) \tag{24}$$

$$P_k = P_{k/k+1} - K_k P_{k/k-1}^{yy} K_k^T \tag{25}$$

4.2.1.5. Step 5: recursive filtering. By inputting the new measurements, steps 1–4 are repeated in the next time step using the updated covariance P_k and Kalman gain K_k.

4.2.1.6. Step 6: prognosis. Then, when the measurement update is terminated, the future $k+1 \ldots n$ step states are predicted within the k-step measures and the time updates from $k+1$ to the desired step (Fig. 5).

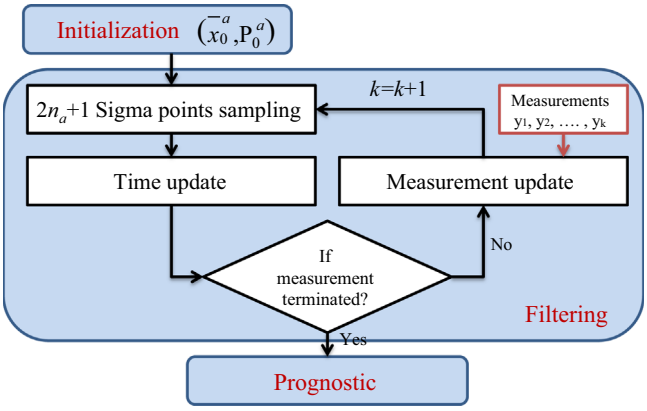

Fig. 5. Flowchart of prognostics using the augmented UKF.

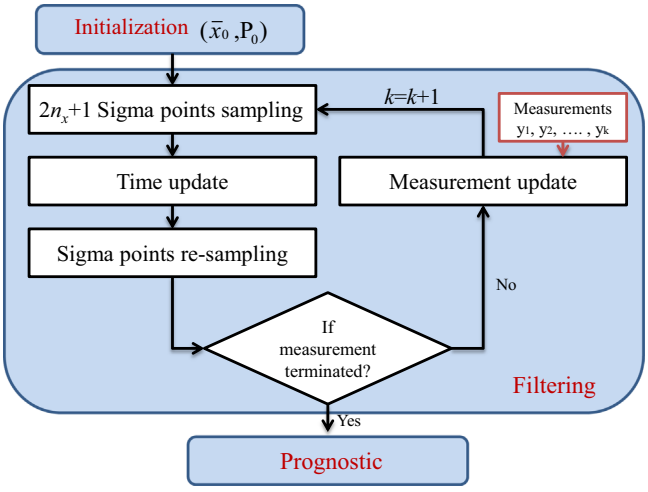

Fig. 6. Flowchart of prognostic using the non-augmented UKF.

4.2.2. Non-augmented UKF

Usually, the computational complexity of the augmented UKF algorithm can be reduced by using the non-augmented form, which can reduce the number of the sigma points as well as the total number of sigma points used ($n_{sigma\ points}=n_x$). Meanwhile, the covariances of the noises are incorporated into the state covariance using a simple additive form [38].

4.2.2.1. Step 1: initialization. The initial state is described by its mean $\bar{x}_0$ and covariance P_0 as defined by Eqs. (6) and (7) shown in the augmented UKF algorithm.

4.2.2.2. Step 2: sigma point sampling. A matrix χ_k with $2n_x+1$ sigma points is generated

$$\chi_{k-1}=[\,\bar{x}_{k-1}\quad \bar{x}_{k-1}+\sqrt{n_x+\lambda^*}\cdot\sqrt{p_{k-1}}\quad \bar{x}_{k-1}-\sqrt{n_x+\lambda^*}\cdot\sqrt{p_{k-1}}\,] \tag{26}$$

where n_x is the number of the state. The composite scaling parameter can be expressed as

$$\lambda^*=\alpha^2(n_x+k)-n_x \tag{27}$$

Then the sigma points are weighted by

$$W_0^{(m)*}=\frac{\lambda^*}{n_x+\lambda^*} \tag{28}$$

$$W_0^{(c)*}=\frac{\lambda^*}{n_x+\lambda^*}+(1-\alpha^2+\beta) \tag{29}$$

$$W_i^{(m)*}=W_i^{(c)*}=\frac{1}{2(n_x+\lambda^*)}\quad i=1,2,\ldots,2n_x \tag{30}$$

4.2.2.3. Step 3: time update. We estimate the transient state $\bar{x}_{k/k-1}$ and measurement $\bar{y}_{k/k-1}$

$$\chi^*_{k/k-1}=f(\chi_{k-1}) \tag{31}$$

$$\bar{x}_{k/k-1}=\sum_{i=0}^{2n_x}W_i^{(m)*}\chi^*_{i,k/k-1} \tag{32}$$

$$P_{k/k-1}=\sum_{i=0}^{2n_x}W_i^{(c)*}[(\chi^*_{i,k/k-1}-\bar{x}_{k/k-1})\cdot(\chi^*_{i,k/k-1}-\bar{x}_{k/k-1})^T]+Q_0 \tag{33}$$

4.2.2.4. Step 4: sigma point re-sampling. We redraw a new set of sigma points to incorporate the effect of the additive process noise.

$$\chi_{k/k-1}=[\bar{x}_{k-1}\quad \bar{x}_{k-1}+\sqrt{n_x+\lambda^*}\cdot\sqrt{p_{k-1}}\quad \bar{x}_{kv1}-\sqrt{n_x+\lambda^*}\cdot\sqrt{p_{k-1}}] \tag{34}$$

$$\xi_{k/k-1}=h(\chi_{k/k-1}) \tag{35}$$

$$\bar{y}_{k/k-1}=\sum_{i=0}^{2n_x}W_i^{(m)*}\xi_{i,k/k-1} \tag{36}$$

4.2.2.5. Step 5: measurement update. The covariance of measurement $P^{yy}_{k/k-1}$ and the cross-covariance of the state and measurement $P^{xy}_{k/k-1}$ is calculated as

$$P^{yy}_{k/k-1}=\sum_{i=0}^{2n_x}W_i^{(c)*}[(\xi_{i,k/k-1}-\bar{y}_{k/k-1})\cdot(\xi_{i,k/k-1}-\bar{y}_{k/k-1})^T]+R_0 \tag{37}$$

$$P^{xy}_{k/k-1}=\sum_{i=0}^{2n_x}W_i^{(c)*}[(\chi_{i,k/k-1}-\bar{x}_{k/k-1})\cdot(\xi_{i,k/k-1}-\bar{y}_{k/k-1})^T] \tag{38}$$

The Kalman gain K_k can be computed by inserting the calculated $P^{yy}_{k/k-1}$ and $P^{xy}_{k/k-1}$ into Eq. (23). The predicted mean $\bar{x}_k$ and covariance P_k can be obtained based on Eqs. (24) and (25), respectively.

4.2.2.6. Step 5: recursive filtering. Like augmented UKF, with inputting the new measurements, the steps 1–4 are repeated for the next time step using the updated covariance P_k and the Kalman gain K_k.

4.2.2.7. Step 6: prognosis. Then, when the measurement update is terminated, the future $k+1\ldots n$ step states are predicted with the k-step measures and the time updates from $k+1$ to the desired step (Fig. 6).

5. Results and discussion

To evaluate our proposed approach, we developed a procedure to compare their prognostic results. The procedure includes four steps: (1) data pretreatment; (2) state initialization; (3) filtering; and (4) prognostics (Fig. 7).

5.1. Data pretreatment

Firstly, we pretreated the raw data collected from the experiment shown in Section 2. We used the lumen flux data sets of the twenty DUTs collected periodically within 10,000 h (1000 h per cycle). After collection, the lumen flux data at each cycle were

normalized to 1 at the 24 h test point for each DUT (as shown in the database [34]; to reduce initial testing errors, this study used the data collected after 24 h initial running as the first test point).

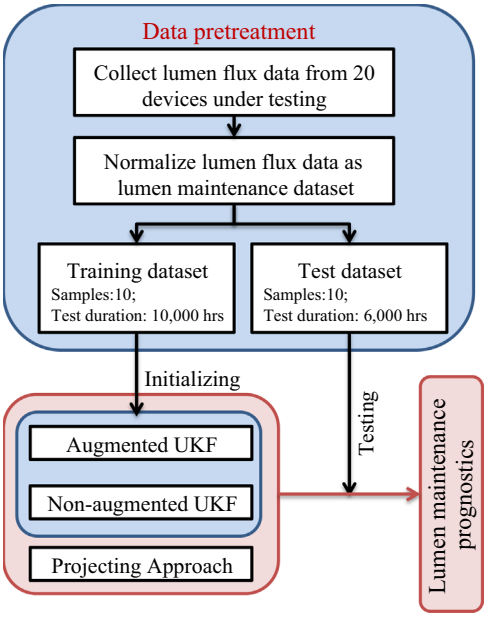

Fig. 7. Lumen maintenance prognostic procedure.

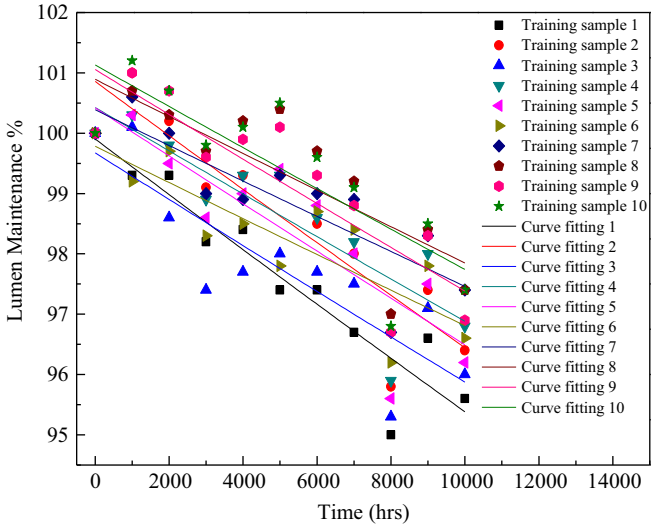

Fig. 8. Nonlinear curve-fitting of lumen maintenance data from training samples.

Then the time series lumen flux data can be transferred to the time series lumen maintenance for each DUT.

Next, all twenty DUTs were separated into two groups: the training samples (ten units) and the test samples (ten units). The calculated lumen maintenance data of the training samples from initial to 10, 000 h were used as the baseline database to train the lumen degradation model, as mentioned in Eq. (2), and initialize the model's parameters. The prognostic performances of proposed models were then compared and evaluated based on the data from the test samples.

As shown in the UKF algorithms (Eqs. (4) and (5)), the measurement model in our case was expressed as the lumen maintenance degradation model (Eq. (2)). The parameters of the degradation model (the fixed effect parameter, A, and the random effect parameter, B) were seen as the states.

$$\text{State model}: \ x_k = [A_k; B_k]$$

$$A_k = A_{k-1} + \nu^A_{k-1} \quad \nu^A_{k-1} \sim N(0, Q^A_v);$$
$$B_k = B_{k-1} + \nu^B_{k-1} \quad \nu^B_{k-1} \sim N(0, Q^B_v); \tag{39}$$

$$\text{Measurement model}: y_k = A_k \cdot \exp(-B_k \cdot 1000 \cdot k) + n_k \tag{40}$$

where k is the measurement cycle (from 0 to 10,000 h).

5.2. State initialization

To begin with, UKF approaches need to initialize the state model with the training dataset. The initial state can be expressed by the parameters of the lumen degradation model of each training sample. These parameters were estimated by the least square curve-fitting approach (Fig. 8) and averaged as the initial states of the test samples, which can be described by the means and covariances (A_0=100.453242, P_{A0}=0.282149945; B_0=3.67271E-06, and P_{B0}=3.42802E-13) (Table 2).

5.3. Filtering

The next step in the UKF approach is the recursive filtering from 1000 to 6000 h, which was conducted to help the updating states with inputting new measurements. Fig. 9 shows the UKF prognostics for the ten test samples, which contains two steps: filtering (from 1000 to 6000 h) and prognosis (from 6000 to 10,000 h). The filtering performances of the two proposed UKF approaches were compared using the mean square error (*MSE*), which is defined as

$$\text{MSE} = \frac{1}{k}\sum_{i=1}^{k}(y_i - \bar{y}_i)^2 \tag{41}$$

where k is the measurement cycle (=6 for the filtering step); and y_i and $\bar{y}_i$ are the real measurements and the estimated values at each measurement cycle, respectively.

Table 2
Parameters of the measurement model obtained from training samples.

No.	*A*	*A_errors*	*B*	*B_errors*	*Adjusted R-square*	*RMSE*
1	99.90392	0.31245	4.63E-06	5.36E-07	0.88053	0.005485
2	100.85699	0.40466	4.47E-06	6.87E-07	0.80568	0.007106
3	99.67384	0.43259	3.89E-06	7.42E-07	0.72512	0.007606
4	100.42592	0.40521	3.59E-06	6.89E-07	0.72361	0.007129
5	100.42186	0.44687	3.99E-06	7.61E-07	0.72658	0.007855
6	99.78427	0.37595	3.02E-06	6.42E-07	0.6792	0.006622
7	100.38776	0.3547	2.96E-06	6.02E-07	0.69818	0.006249
8	100.89255	0.43315	3.06E-06	7.32E-07	0.62367	0.007629
9	101.05469	0.43391	3.70E-06	7.34E-07	0.71035	0.007632
10	101.13062	0.47028	3.41E-06	7.94E-07	0.63641	0.008277
Average	100.453242	0.406977	3.67271E-06	6.91877E-07	0.720933	0.007159
Covariance	0.282149945	0.002256063	3.42802E-13	6.20757E-15	0.005742824	7.00137E-07

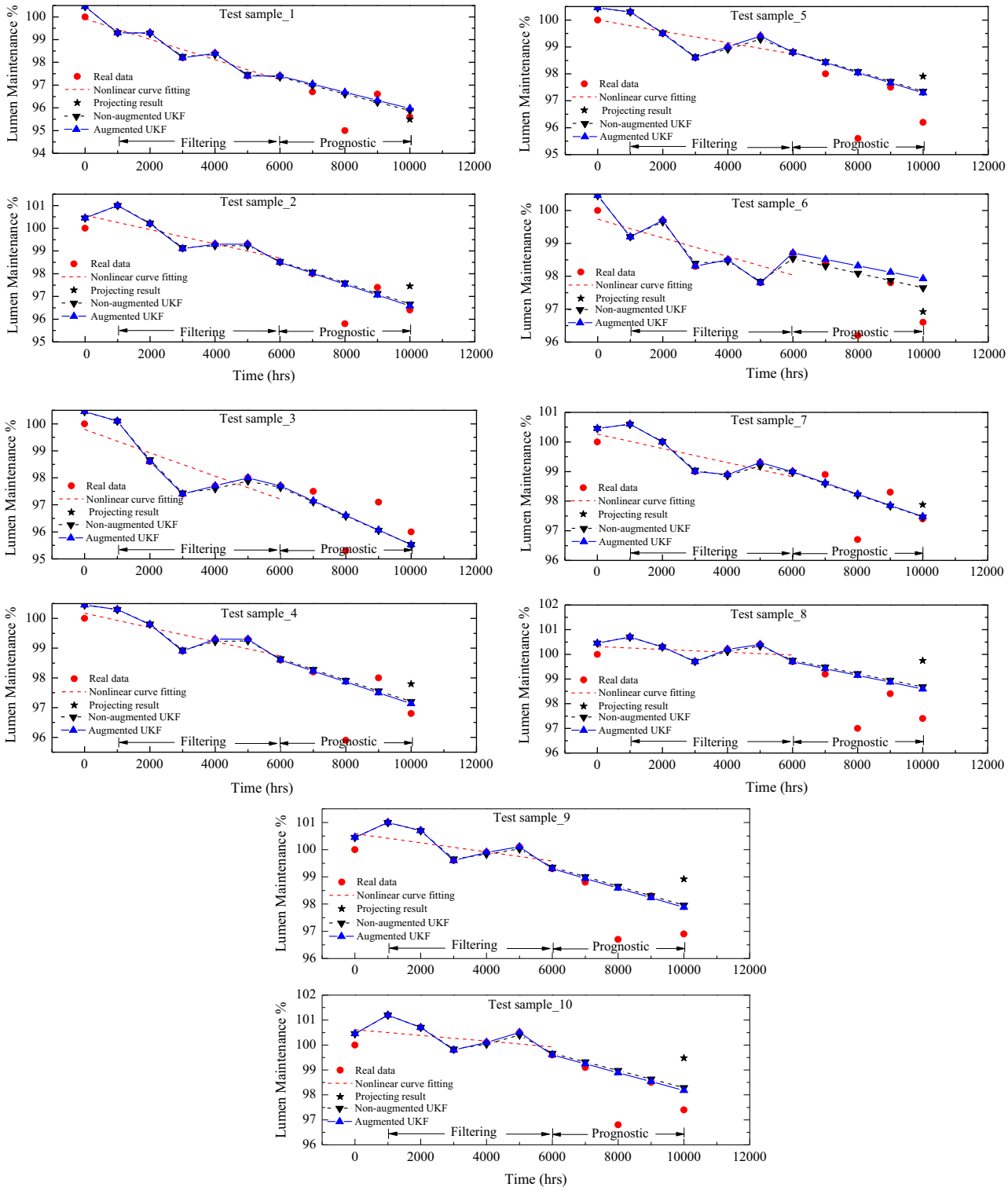

Fig. 9. Lumen maintenance prognostics with UKF approaches for test samples (Test samples_1–10).

The calculated MSE values of the two UKF approaches of each test sample are shown in Fig. 10. The MSE values of the non-augmented UKF is nearly 400–1500 times larger than that of the augmented UKF, which indicates that the augment UKF has a better estimation performance than the non-augmented UKF. As discussed in Section 3, in order to keep the accuracy of the state estimation, both of the UKF approaches consider the effect of process noise into the state model; however, the difference between these two approaches is that the augmented UKF supposes that the noises are non-additive and can be inserted into the sigma sampling step in recursion, while the non-augmented UKF just uses the re-sampling method with additive noises. The superiority of the augmented UKF approach can be attributed to its capacity in capturing and propagating the odd-order moment information through one filtering recursion. Mathematically, the augmented UKF approach can capture more statistical information by introducing the effect of process and measurement noises into both

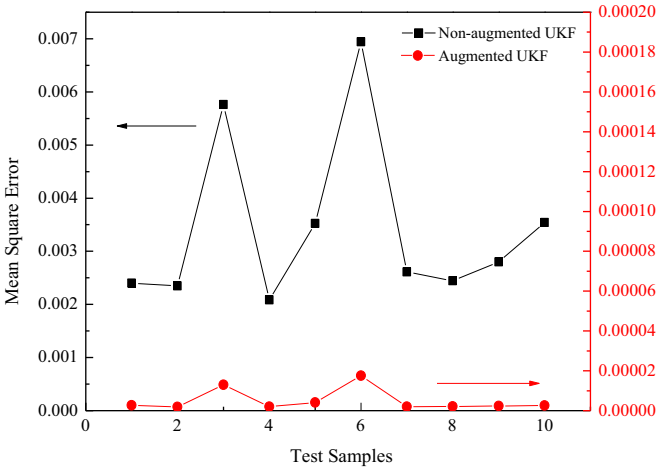

Fig. 10. Mean square errors of UKF filtering step.

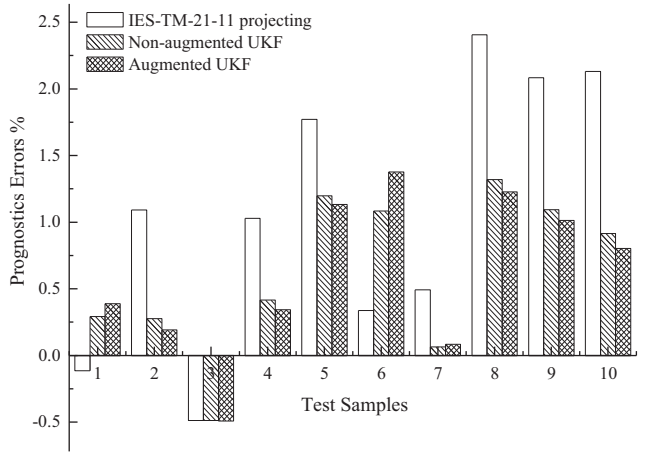

Fig. 11. Lumen maintenance prognostics errors at 10,000 h.

the state and measurement updating non-additively, which will reduce errors between the estimations and the actual measurements.

5.4. Prognostics

After the recursive filtering steps in both UKF approaches, the lumen maintenance of each test sample at 10,000 h was predicted, as shown in Fig. 9. At the same time, following the projection procedure shown in Section 3.1, the lumen maintenance of test samples at 10,000 h were also extrapolated by the IES-TM-21-11 projection approach (marked by black stars in Fig. 9).

To evaluate the prognostic performance of the above mentioned approaches, we used both accuracy-based and precision-based metrics [39]. The accuracy-based metric is defined as the deviation between prognostics results and real measurements, which can be expressed as the prognostics errors (*Pe*):

$$Pe_k = \frac{\overline{y}_k - y_k}{y_k} \times 100\% \tag{42}$$

where $\overline{y}_k$ and y_k are the prognostics results and actual measurements of the lumen maintenance at the kth cycle, respectively. The measurement cycle k is 10 for the prognostics step in this study.

Fig. 11 shows the lumen maintenance prognostics errors of the test samples. For the majority of the test samples (samples 2, 4, 5, 7–10), compared to the IES-TM-21-11 projecting approach, both UKF approaches had lower prognostics errors and increase the prognostic accuracy. However, the UKF approach lost its superiority in samples 1, 3, and 6. In fact, the accuracy of UKF-based prognostics is determined by the last estimated state after recursive filtering (the state at 6000 h for this paper). The projecting results from using the IES-TM-21-11 approach, however, are affected by the least square estimation, which depends on the minimization of the sum of the residuals between the actual measurements and the calculated values (as shown in Appendix A). The differences between the least squares method and the UKF approach are discussed in [19,40]. Firstly, the UKF deals with dynamic stochastic systems, while the least squares method is used for deterministic systems. Secondly, the UKF updates system states recursively by absorbing new measurements, while the least squares implementation uses batch processing.

Table 3
Performances of prognostic approaches.

Approaches	Prognostic errors mean *E* (*Pe*) (%)	Prognostic errors variance *Var* (*Pe*)
IES-TM-21-11 projecting	1.07	1.015E-4
Non-augmented UKF	0.62	3.505E-5
Augmented UKF	0.61	3.585E-5

Besides accuracy-based metrics, we also chose a precision-based metric, which is considered to be an evaluator of the stability of a prognostic model. The precision-based metric is derived from the mean ($E(Pe)$) and variance ($Var(Pe)$) of prognostic errors within a set of test samples.

$$E(Pe) = \frac{1}{N}\sum_{i=1}^{N} Pe_{10}^{i} \tag{43}$$

$$Var(Pe) = \frac{1}{N}\sum_{i=1}^{N} [Pe_{10}^{i} - E(Pe)]^2 \tag{44}$$

Table 3 lists the means and variances of prognostic errors from the above mentioned approaches, which indicates that both the two proposed UKF approaches have the similar prognostic performance for all test samples, with lower mean and variance of the prognostic errors. This means that compared to the IES-TM-21-11 projecting approach, both of the two UKF approaches are effective methods for nonlinear prediction, although they have different estimation performance in filtering step. From author's view, the elements to determine the final prognostic performance of the proposed UKF methods can be summarized as: (1) initial state [41]; (2) measurement data; and (3) filtering (recursive updating with UT algorithm). Based on the same initial state and measurement data, the estimation errors produced in the filtering step from both augmented and non-augmented UKFs are too small to affect the final prognostic results (MSE non-augmented < 0.007; MSE_augmented < 0.00002, Fig. 10). It also indicates that the UKF methods have more robust prognostic performance than the least-square regression used in IES-TM-21-11 projecting approach.

6. Conclusions

In this paper, we imported a “prognostic” concept to qualification testing and built a prognostic-based qualification test model for high power white LEDs (HPWLEDs). To increase the prediction accuracy, we presented a nonlinear filter-based prognostic approach (the recursive Unscented Kalman Filter) to predict the lumen maintenance of HPWLEDs based on the short-term observed data. The prognostic performance of the proposed approach and the IES projecting approach were also compared

and evaluated with both accuracy- and precision-based metrics. The following conclusions can be drawn from these results.

(1) The recursive UKF-based prognostic approach can be expressed as two steps: filtering and prognostics. With time and measurement updates, the states can be estimated and forwarded dynamically. This study defined the parameters of the lumen degradation model as the dynamic states, and they can be updated and optimized recursively within the UKF algorithm.
(2) Two types of UKF algorithm, the augmented UKF and the non-augmented UKF, were used in this study. The filtering results showed that the augmented UKF produced a better estimation than the non-augmented UKF did, because it captured more statistical information by introducing the effect of process and measurement noises into both state and measurement updating non-additively. However, the non-augmented UKF is easier to implement with less calculation.
(3) The prognostic results of the proposed approaches were evaluated based on both accuracy- and precision-based metrics, and indicated that both UKF approaches can increase the prediction accuracy for the majority of test samples and they possess higher prediction precision and more robust prognostic performance compared to the IES-TM-21-11 projecting approach.

Based on above findings, there is still some work should be done in the future: (1) predicting long-term lumen maintenance ($>10{,}000$ h); (2) estimating remaining useful life, which can be defined as the time when the predicted lumen maintenance falls under the failure threshold (50% for the display lightings and 70% for the general lighting); and (3) to reduce the manual measurement errors and improve prognostic performance, an online measurement, diagnostic and the prognostic system with the proposed UKF methods will be investigated for the LED qualification test in the future work.

Acknowledgments

The work described in this paper was partially supported by a grant from the Research Committee of The Hong Kong Polytechnic University and was also partially supported by a grant from the Research Grants Council of the Hong Kong Special Administrative Region, China (CityU8/CRF/09).

Appendix A. Least Squares Estimation

Supposing that a set of n data points (t_1, y_1), (t_2, y_2),…, (t_n, y_n) follows an exponential model (A.1) and their transferred data set (t_1, ζ_1), (t_2, ζ_2),…, (t_n, ζ_n) can be fitted by a least square straight line defined as (A.2):

$$y = A \cdot \exp(-B \cdot t) \tag{A.1}$$

$$\zeta = \ln A - B \cdot t \tag{A.2}$$

where $\zeta = ln(y)$.

Through minimizing the sum of the squares of the residuals between actual measurements and calculated values (A.3), the parameters of the exponential model (A.1) can be estimated as follows:

$$\min_{A;B}\left\{\frac{1}{n}\sum_{i=1}^{n}[\zeta^i - (\ln A - B \cdot t^i)]^2\right\} \tag{A.3}$$

$$B = \frac{\sum_{i=1}^{n} t_i \sum_{i=1}^{n} \zeta_i - n \sum_{i=1}^{n} t_i \zeta_i}{n \sum_{i=1}^{n} t_i^2 - \left(\sum_{i=1}^{n} t_i\right)^2} \tag{A.4}$$

$$A = \exp\left(\frac{\sum_{i=1}^{n} \zeta_i - B \sum_{i=1}^{n} t_i}{n}\right) \tag{A.5}$$

References

[1] Schubert EF, Kim JK. Solid-state light sources getting smart. Science 2005;308:1274–8.
[2] Schubert EF. Light-emitting Diodes. 2nd ed.. Cambridge: Cambridge University Press; 2006.
[3] Mottier P. LEDs for Lighting Applications. USA: John Wiley & Sons, Inc.; 2009.
[4] Lenk R, Lenk C. Practical Lighting Design with LEDs. New Jersey: John Wiley & Sons, Inc.; 2011.
[5] IES-LM-79-08. Electrical and Photometric Measurements of Solid-State Lighting Products. USA: Illuminating Engineering Society; 2008.
[6] IES-LM-80-08. Approved Method for Lumen Maintenance Testing of LED Light Source. USA: Illuminating Engineering Society; 2008.
[7] ANSI_NEMA_ANSLG C78.377-2008. Specifications for the Chromaticity of Solid State Lighting Products: for electric lamps. USA: American National Standard Lighting Group; 2008.
[8] ANSI_ANSLG C78.377-2011. Specifications for the Chromaticity of Solid State Lighting Products: for electric lamps. USA: American National Standard Lighting Group; 2011.
[9] Fan JJ, Yung KC, Pecht M. Physics-of-failure-based prognostics and health management for high-power white light-emitting diode lighting. IEEE Trans Device Mater Reliab 2011;11:407–16.
[10] Fan JJ, Yung KC, Pecht M. Lifetime estimation of high-power white LED using degradation-data-driven method. IEEE Trans Device Mater Reliability 2012;12:470–7.
[11] IES-TM-21-11. Projecting Long Term Lumen Maintenance of LED Light Sources. USA: Illuminating Engineering Society; 2011.
[12] ASSIST Recommendation. LED Life for General Lighting; Lighting Research Center: New York:Troy; 2005.
[13] DR04: LM-80 Test Report, Luxeon, Philps, 2011.
[14] Cree® LED Components IES LM-80-2008 Testing Results (Revision:12), CREE, December 6; 2012. ⟨http://www.cree.com/XLAMP⟩.
[15] Pecht M. Prognostics and Health Management of Electronics. New Jersey: John Wilely & Sons, Inc.; 2008.
[16] Daigle M, Saha B, Goebel KA. Comparison of filter-based approaches for model-based prognostics. In: proceedings of the 2012 IEEE aerospace conference; 2012.
[17] Yang SK, Liu TS. State estimation for predictive maintenance using Kalman filter. Reliab Eng Syst Saf 1999;66:29–39.
[18] Yang SK. An experiment of state estimation for predictive maintenance using Kalman filter on a DC motor. Reliab Eng Syst Saf 2002;75:103–11.
[19] Gibbs B. Advanced Kalman Filtering, Least-Squares and Modeling. New Jersey: John Wilely & Sons, Inc.; 2011.
[20] Simon D. Optimal state estimation : Kalman H, editor [infinity] and nonlinear approaches. New Jersey: John Wilely & Sons, Inc.; 2006.
[21] Zio E, Peloni G. Particle filtering prognostic estimation of the remaining useful life of nonlinear components. Reliab Eng Syst Saf 2011;96:403–9.
[22] Julier SJ, Uhlmann JK. Unscented filtering and nonlinear estimation. Proc IEEE 2004;92:401–22.
[23] Julier SJ, Uhlmann JK, Durrantwhyte HF. A new approach for filtering nonlinear systems. In: Proceedings of the 1995 american control conference. vol. 1–6; 1995, pp. 1628–1632.
[24] Wan EA, van der Merwe R. The Unscented Kalman Filter for nonlinear estimation. In: IEEE 2000 adaptive systems for signal processing, communications, and control symposium – proceedings; 2000, pp. 153–158.
[25] Kim J, Vaddi SS, Menon PK, Ohlmeyer EJ. Comparasion between nonlinear filtering techniques for spiraling ballistic missile state estimation. IEEE Trans Aerosp Electron Syst 2012;48(1):313–28.
[26] Hu SQ, Jing ZL. The Principle Particle Filter and its Application. Beijing: Science Press; 2010.
[27] Santhanagopalan S, White RE. State of charge estimation using an unscented filter for high power lithium ion cells. Int J Energy Res 2010;34:152–63.
[28] Lall P, Lowe R, Goebel K. Prognostics health management of electronic systems under mechanical shock and vibration using Kalman filter models and metrics. IEEE Trans Ind Electron 2012;59:4301–14.
[29] Jafarzadeh S, Lascu C, Fadali MS. State estimation of induction motor drives using the Unscented Kalman Filter. IEEE Trans on Ind Electron 2012;59:4207–16.
[30] Technical Datasheet DS56, Luxeon, Philps, 2008.
[31] Liu ZY, Liu S, Wang K. Status and prospects for phosphor-based white LED packaging. Front Optoelectron China 2009;2(2):119–40.

[32] Luo H, Kim JK, Schubert EF, Cho J, Sone C, Park Y. Analysis of high-power packages for phosphor-based white-light-emitting diodes. Appl Phys Lett 2005:86.
[33] Ye S, Xiao F, Pan YX, Ma YY, Zhang QY. Phosphors in phosphor-converted white light-emitting diodes Recent advances in materials, techniques and properties. Mat Sci Eng R. 2010;71:1–34.
[34] DR03: LM-80 Test Report, Luxeon, Philps, 2010.
[35] Lu CJ, Meeker WQ. Using degradation measures to estimate a time-to-failure distribution. Technometrics 1993;35(2):161–74.
[36] Ishizaki S, Kimura H, Sugimoto M. Lifetime estimation of high power white LEDs. J Light Vis Environ 2007;31(1):15.
[37] Narendran N, Gu Y, Freyssinier JP, Yu H, Deng L. Solid-state lighting: failure analysis of white LEDs. J. Cryst. Growth 2004;268(3–4):449–56.
[38] Wu YX, Hu DW, Wu MP, Hu XP. Unscented Kalman filtering for additive noise case: augmented vs. non-augmented. ACC. In: Proceedings of the 2005 american control conference,vol. 6; 2005, pp. 4051–40555.
[39] Saxena A., Celaya J., Balaban E., Goebel K., Saha B., Saha S., et al. Metrics for Evaluating Performance of Prognostic Techniques. In: Proceedings of the 2008 international conference on prognostics and health management (Phm); 2008, pp. 174–190.
[40] Sorenson HW. Least-Squares Estimation – from Gauss to Kalman. IEEE Spectrum 1970;7:63–8.
[41] Fan J.J., Yung K.C., Pecht M. Prognostics of Chromaticity State for Phosphor-converted White Light Emitting Diodes Using an Unscented Kalman Filter Approach. IEEE Trans Device Mater Reliab, http://dx.doi.org/ 10.1109/TDMR.2013.2283508.

The author has requested enhancement of the downloaded file. All in-text references underlined in blue are linked to publications on ResearchGate.